Review Article

The current and future role of magnetic resonance imaging in prostate cancer detection and management

Jan Philipp Radtke[1,2], Dogu Teber[1], Markus Hohenfellner[1], Boris A. Hadaschik[1]

[1]Department of Urology, Heidelberg University Hospital, Heidelberg, Germany; [2]Department of Radiology, German Cancer Research Center, Heidelberg, Germany

Correspondence to: Professor Boris A. Hadaschik. Deputy Clinical Director, Department of Urology, Heidelberg University Hospital, Im Neuenheimer Feld 110, 69120 Heidelberg, Germany. Email: boris.hadaschik@med.uni-heidelberg.de

Purpose: Accurate detection of clinically significant prostate cancer (PC) and correct risk attribution are essential to individually counsel men with PC. Multiparametric MRI (mpMRI) facilitates correct localization of index lesions within the prostate and MRI-targeted prostate biopsy (TPB) helps to avoid the shortcomings of conventional biopsy such as false-negative results or underdiagnosis of aggressive PC. In this review we summarize the different sequences of mpMRI, characterize the possibilities of incorporating MRI in the biopsy workflow and outline the performance of targeted and systematic cores in significant cancer detection. Furthermore, we outline the potential of MRI in patients undergoing active surveillance (AS) and in the pre-operative setting.

Materials and methods: An electronic MEDLINE/PubMed search up to February 2015 was performed. English language articles were reviewed for inclusion ability and data were extracted, analyzed and summarized.

Results: Targeted biopsies significantly outperform conventional systematic biopsies in the detection of significant PC and are not inferior when compared to transperineal saturation biopsies. MpMRI can detect index lesions in app. 90% of cases as compared to prostatectomy specimen. The diagnostic performance of biparametric MRI (T2w + DWI) is not inferior to mpMRI, offering options to diminish cost- and time-consumption. Since app 10% of significant lesions are still MRI-invisible, systematic cores seem to be necessary. In-bore biopsy and MRI/TRUS-fusion-guided biopsy tend to be superior techniques compared to cognitive fusion. In AS, mpMRI avoids underdetection of significant PC and confirms low-risk disease accurately. In higher-risk disease, pre-surgical MRI can change the clinically-based surgical plan in up to a third of cases.

Conclusions: mpMRI and targeted biopsies are able to detect significant PC accurately and mitigate insignificant PC detection. As long as the negative predictive value (NPV) is still imperfect, systematic cores should not be omitted for optimal staging of disease. The potential to correctly classify aggressiveness of disease in AS patients and to guide and plan prostatectomy is evolving.

Keywords: Prostate cancer (PC); magnetic resonance imaging (MRI); multiparametric MRI (mpMRI); MRI/TRUS-fusion-guided biopsy; staging; targeted prostate biopsy (TPB); systematic biopsy (SB); radical prostatectomy (RP); PIRADS v1.0; PIRADS v2.0

Submitted Mar 22, 2015. Accepted for publication May 26, 2015.
doi: 10.3978/j.issn.2223-4683.2015.06.05
View this article at: http://dx.doi.org/10.3978/j.issn.2223-4683.2015.06.05

Introduction

Prostate cancer (PC) is the most common noncutaneous malignancy in men in Western countries (1). In 2011, around 900,000 new cases and among 250,000 deaths were recorded worldwide (1). According the European Association of Urology guidelines an elevated prostate specific antigen (PSA)-level should trigger an extended 12-core systematic TRUS-guided biopsy, which is endorsed as the optimal biopsy method (2). This diagnostic strategy is based on random sampling and is largely operator dependent. Consecutively, this biopsy technique is subject to sampling error and provides poor characterization of PC aggressiveness (3). The main shortcomings of the 12-core TRUS biopsy technique are failure to detect clinically significant cancer and imprecise PC risk stratification (undersampling) and detection of small low-risk clinically insignificant cancers (overdetection) (4,5). This diagnostic uncertainty can lead to repeat biopsy, delayed detection of significant disease or disease overtreatment. The need of precise tumor detection and staging increases in the context of recent trends of active surveillance (AS) and focal therapy.

Since its first usage in 1983, magnetic resonance imaging (MRI) is increasingly used for PC diagnosis because of growing availability and multiparametric imaging, combining anatomic and functional data (6). A number of studies confirm the diagnostic reliability of multiparametric MRI (mpMRI) for PC detection (4,7). In the past, widespread acceptance of mpMRI suffered from a lack of standardized diagnostic criteria for reporting of results, leading to a substantial variability in interpretation (8). To standardize the evaluation and reporting of prostate MRI, the European Society of Urogenital Radiology (ESUR) published guidelines based on an expert consensus in 2012, termed the Prostate Imaging Reporting and Data System (PIRADS) (9). This guideline provides explicit and standardized criteria for Likert-scoring of multiparametric sequences [T2w, diffusion-weighted imaging (DWI), dynamic contrast enhanced imaging (DCE) and MR-spectroscopy] (9). Since then, the PIRADS score has been externally validated with a good accuracy, suggesting that this 5-point-Likert scoring allows to detect PC accurately (10-13). The T2w, DWI and DCE sequences have been maturating as being most accurate for PC detection, whereas the use of MR-spectroscopy has mostly been abandoned.

The accuracy of mpMRI and PIRADS scoring has not only been established for biopsy specimen, but also for histopathologic correlation using prostatectomy specimen. In the pre-PIRADS era, Isebaert *et al.* found a sensitivity of 58.5% for PC detection (14). Recent publications demonstrate detection rates of significant PC between 80-96% for MRI compared to whole-mount sections (15-17).

MRI-targeted biopsies (TB) can be taken by various approaches. Visual estimation (VE) allows the adaptation of TB in clinical practice without costs for new equipment, but lacks real-time feedback regarding accuracy. The effectiveness and accuracy of VE biopsy vary among studies. Haffner *et al.* detected significant PC in 43% of men using TB and missed only 5.2% of significant PC as compared to standard biopsy (18). In addition, Kasivisvanathan *et al.* reported non-inferiority of VE TB as compared to transperineal mapping (19). However, the performance of VE TB is strongly experience dependent, limiting the widespread of this approach (3). In-bore MRI guided biopsy is an alternative, offering a cancer detection rate (CDR) of 41% and finding mostly clinically significant PC (20). These results have been corroborated by recent studies, demonstrating that in-bore MRI guided biopsy is a feasible technique, requiring fewer cores to detect similar rates of significant cancer and a median detection rate for all PC around 42% (21,22). However, the use of in-bore TB alone might be critical as several studies demonstrate that app. 10% of significant tumors are MRI-invisible (12,13,23,24). MRI/TRUS-fusion-guided biopsies with software-registration potentially overcome limitations of cognitive fusion through reproducible methods of identifying MRI lesions on ultrasound (25). The utility of TB versus systematic biopsy (SB) has recently been established in a large cohort that has been analysed according to standards formulated by an international consensus meeting (26,27). Siddiqui *et al.* published the results of 1,003 patients undergoing MRI-TB of MRI-visible lesions in addition to standard 12-core biopsy (26). In their study, TB detected significantly more (30%, P<0.001) high-risk PC and 17% fewer low-risk PC (P=0.002) compared to SB (26). However, TB alone missed 8.1% of intermediate- and high-risk PC compared to the combination of TB and SB. Moreover, when compared to prostatectomy specimen the negative predictive value of TB to exclude significant disease was still imperfect (70%). Furthermore, when TB were compared to a different reference test (24-core transperineal SB), 20.9% of significant PC were detected by TB alone, whereas 12.8% were missed by TB alone (12). Overall, no statistically significant difference in significant PC detection occurred between both approaches (12). In conclusion, for optimal staging both TB and SB should be taken to detect significant PC accurately, echoing other

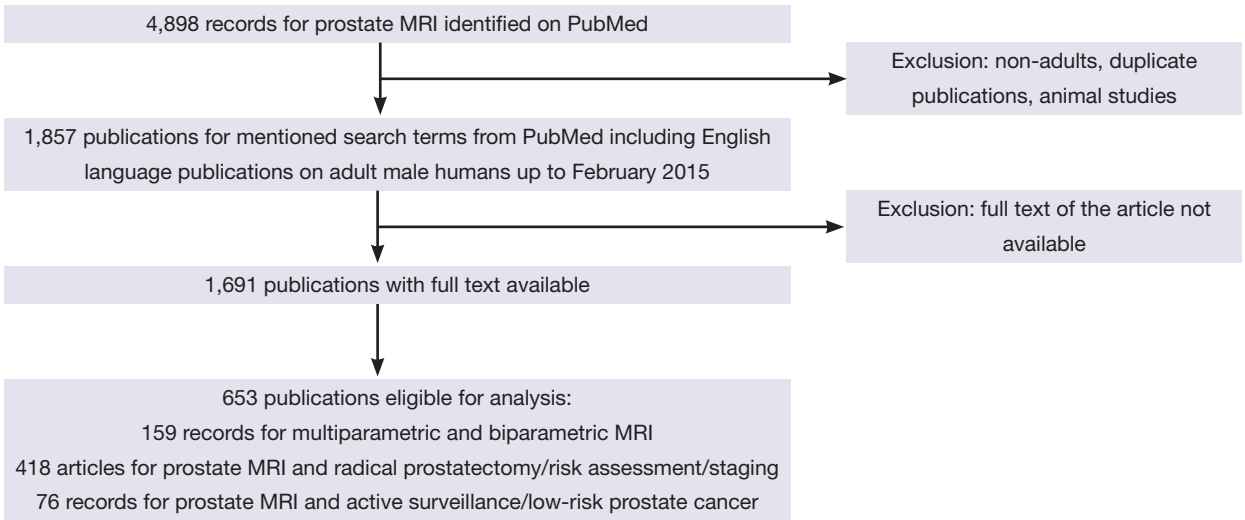

Figure 1 Study flowchart with inclusion and exclusion criteria for manuscripts into analysis. MRI, magnetic resonance imaging.

recent publications (12,24).

MpMRI also has the potential to predict extracapsular extension (ECE) on radical prostatectomy (RP) (28). Somford *et al.* and Marcus *et al.* have demonstrated promising negative (NPV) and positive predictive values (PPVs) of ECE and the possibility of changing the surgical strategy (28,29).

In this review we evaluate the role of MRI in the pre-biopsy setting and the utility to predict RP outcome. Moreover we describe the different MRI sequences and biopsy techniques.

Materials and methods

We searched MEDLINE/PubMed for English language manuscripts published up to February 2015 using the following search terms: MRI, multiparametric MRI, biparametric MRI, MRI-guided, MRI-targeted, image-guided, MRI-ultrasound fusion, cognitive, prostate, PC, biopsy, detection, AS, risk assessment, risk stratification, PIRADS, NMR, cancer detection, visual estimation and extraprostatic extension (EPE). Non-English articles were excluded from analysis. Inclusion criteria were male gender, adult and availability of full text. Overall, 653 publications were included. Data were extracted and analyzed.

The literature search and study pre-selection is graphically displayed in *Figure 1*.

Results

Limitations of the contemporary systematic biopsy technique

False-negative biopsy

Standard 12-core transrectal biopsies need optimal spatial distribution for tumor detection and are consequently subject to sampling error. Undersampling occurs in up to 30-80% of patients with significant PC (4,26,30). Especially cancers with small volume or PC located in the transition zone (TZ) and anterior prostate are difficult to detect by random 12-core transrectal approaches (31,32). Additionally larger glands are subject to greater risk of false-negative biopsy (30). To overcome this sampling error, multiple repeat biopsies are often performed. However, these can result in overdetection of indolent cancers that may not have caused harm (3).

Incorrect risk stratification

The undersampling of the prostate during systematic transrectal procedures can lead to incorrect risk stratification of PC. More strict definitions of PC do not only include the Gleason score (GS) (≥3+4 or ≥4+3), but also the lesion volume (33,34). Random biopsies risk inadequate lesion sampling, as the cancer core length is significantly decreased compared to TB (35,36). This may reveal a small length of tumor in a core with a low GS, when in fact a significant lesion may occur adjacent to the biopsy location (3,37).

Another risk of conventional TRUS-guided biopsy is upgrading. Dinh *et al.* recently analyzed a SEER-database cohort of 10,273 patients, and found an upgrading of 44% from clinically low-risk PC in biopsy to GS ≥7 in RP specimen (38). Shaw *et al.* also found an upgrading of 50.2% from low-risk PC to intermediate- and high-risk PC in RP specimen analyzing 848 patients (39).

Detection of clinically insignificant disease

Approximately 60% of men over age of 80 years harbor clinically insignificant PC without suffering from it at autopsy studies (40). These clinically insignificant PC are often identified by chance during a SB and may contribute to overdetection and overtreatment of indolent PC (5,41,42).

Risk of infection

Although the TRUS-biopsy approach is the standard diagnostic approach for over 20 years, significant side-effects and morbidity are rising, especially post-biopsy infections (43). In a national Swedish cohort of 51,321 men, Lundström *et al.* showed an infection rate of 6% after transrectal biopsy (44). Prevention and prophylaxis from infections caused by rectal milieu is especially important, since the frequency of Escherichia coli resistant to fluoroquinolone increased from 11% in 2006 to 13% in 2011 (44,45). Additionally, Feliciano *et al.* described not only a fluorquinolone resistance of Escherichia coli, but also to gentamicin (22% of cases), trimethoprim/sulfamethoxazole in 44%, piperacillin in 72% and ampicillin in 94% (46). Furthermore Cohen *et al.* described an initial fluoroquinolone resistance of Escherichia coli in 24.4% of cases in an initial biopsy cohort of 416 men (47).

Transperineal approach

The transperineal approach is an alternative to the transrectal entry path, causing less risk of infection. Additionally, the anterior prostate is easier to access. Furthermore, transperineal mapping biopsy specimen undergo significantly less upgrading on RP specimen (8% versus 52% in a publication of Crawford *et al.*) (48). One disadvantage is that transperineal biopsies are more painful. Thus, anesthesia is needed, especially in case of saturation or mapping biopsies averting the wide-spread use of this approach.

Extended systematic and saturation biopsies

The debate on the optimal number of biopsy core samples that should be taken is still open. Ploussard *et al.* have demonstrated that an increase from 12 to 21 cores significantly increases the detection rate of significant PC (49). Transperineal mapping biopsy (TPMB) aims for optimal staging and detection of all significant PC by using an external grid of 5 mm (50,51). Lecornet *et al.* have shown that TPMB detects nearly all significant PC lesions above 0.5 mL (52). However, TPMB is significantly more invasive than SB leading to urinary retention and the potential for oversampling of clinically insignificant PC, which often results in overtreatment. Valerio *et al.* report that, beside an accurate index lesion detection, insignificant PC was detected in up to 42.9% of TPMB (53). Additionally, the prostate is mobile, deformable and swells during biopsy, so real-time sampling errors in vivo might still occur (25). Thus, Ukimura *et al.* conclude that the specific clinical indication for TPMB, remains under debate (25).

Prostate mpMRI for PC detection and localization

The first application of prostate MRI was published by Hricak *et al.* in 1983 (54). Since then, the field strength of MRI increased from 0.35 Tesla (T) to 3T and standardized multiparametric sequences (T2w, DWI and DCE) were established. MRI and TB detect more clinically significant PC compared to standard 12-core TRUS-biopsy (4,26,37,55). To establish a standardized MRI technique and a quantitative structured reporting system, the ESUR promoted the ESUR guidelines in 2012 (9). In 2015, a revised PIRADS version was published by the American College of Radiologists (56). The imaging techniques are described in the following sections.

T2-weighted imaging

T2w MR images have high spatial resolution and clearly define the prostate's zonal anatomy (*Figure 2*) (59). PC in the peripheral zone often appear as a low signal intensity area on T2w (9). The degree of intensity decrease differs with the GS, with higher GS components showing lower signal intensities (60). However, T2w imaging can result in false positive findings, as low-signal intensity also occurs in acute and chronic prostatitis, atrophy, scars, post-irradiation, hyperplasia and post-biopsy hemorrhage (3). Because of the heterogeneous appearance of benign prostate hyperplasia with both, increased and decreased signal intensity, PC in the TZ can be difficult to distinguish from benign tissue (61,62). Morphologic features such as homogeneously low signal intensity, irregular edges of the suspicious lesion, invasion into the urethra or the anterior fibromuscular stroma

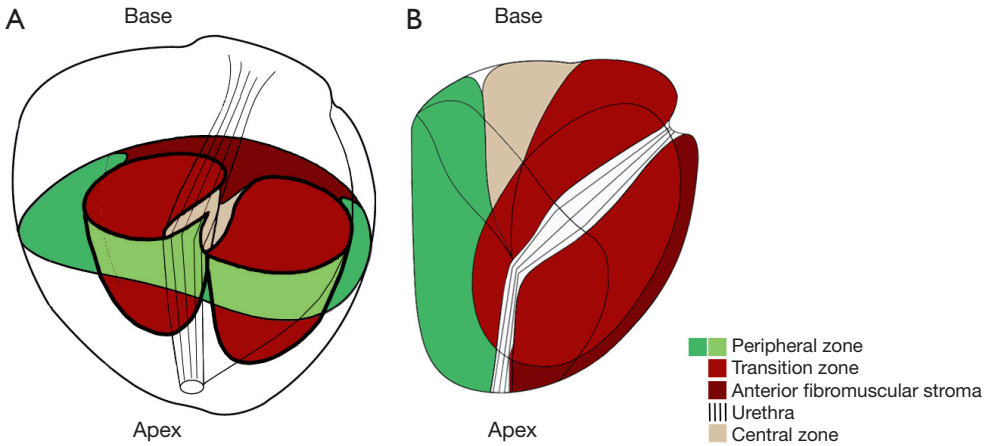

Figure 2 Scheme of prostate zones. Transversal (A) and sagittal (B) scheme of prostate zones, according to McNeal *et al.* and adapted from Bouyé *et al.* (57,58). The dark red colored area represents the anterior fibromuscular stroma and the bright red colored area the TZ of the prostate (57,58). The peripheral zone is colored in green, the central zone in beige. TZ, transition zone.

(AFMS), and lenticular shape are helpful for detection of TZ tumors (63). Moreover, the updated PIRADS guidelines state that T2w Imaging is the dominant sequence for the TZ [*Table 1* (see part A) and *Table 2*] (56).

Diffusion-weighted imaging (DWI)

DWI is based on Brownian motion and measures random motion of water molecules. The strength of the gradient that determines the degree of diffusion-weighting is reflected by the sequence's b value. Performing DWI with multiple b values, it is possible to compute the apparent diffusion coefficient (ADC) based on the signal intensity measured at each b value image to quantify the restriction of water diffusion. B values of 0, 100 and 800-1,000 s/mm^2 are recommended (9). For ADC calculation, the highest b value should be 1,000 s/mm^2 (9). The utility of higher b values up to 2,000 s/mm^2 is under debate (64,65). On ADC maps, PC frequently shows low ADC values and an inverse correlation exists between quantitative ADC values and the GS (65-67). While ADC does correlate with GS, the confidence intervals are widely overlapping, limiting the ability to use ADC as a surrogate of GS (3,67).

Limitations of DWI include low signal-to-noise ratio and image distortion, both of which become more problematic at higher b values (3). Nonetheless, DWI is a widely available technique, and given its association with tumor aggressiveness, it may prove to be the primary sequence for tumor detection and characterization, especially in the peripheral zone, were it is recommended as the dominant sequence [*Table 1* (see part B) and *Table 2*] (56,67).

Dynamic contrast-enhanced imaging and role of biparametric MRI

Dynamic contrast-enhanced MRI consists of a series of fast T1w-sequences covering the prostate, before and after a bolus injection of gadolinium chelate (9). It is the most common imaging method for evaluation of tumor vascularity (68). As many other malignancies, PC often demonstrate early enhancement compared to normal tissue (69). However, kinetics of PC enhancement can be variable and heterogeneous (56). Recent guidelines recommend to include DCE not to miss some small significant PC (56). If focal lesions are found, T2w and DWI images should be carefully interrogated for corresponding abnormalities (56). At present, the additional value of DCE is discussed controversially. Some publications state that addition of DCE and/or DW imaging to T2-weighted MRI significantly improved sensitivity from 63% to 79-81% in the peripheral zone, while maintaining a stable specificity (7). Yoshizako *et al.* demonstrated that the combined use of DWI, DCE, and T2-weighted MRI increased the accuracy in detection of TZ cancer compared to T2w alone, from 64% to 79% (70). The PIRADS 2015 guidelines still recommend the use of DCE, whereas Rosenkrantz *et al.*, Hoeks *et al.*, Rais-Bahrami *et al.* and Schimmöller *et al.* postulate that additional DCE did not improve the detection and localization accuracy of significant PC in all zones and especially in the TZ (56,62,71-73). When performed, DCE is positive when there is enhancement that is focal, earlier or contemporaneous with enhancement of adjacent normal prostatic tissue and usually corresponding

Table 1 PIRADS scoring for (A) T2w imaging, (B) DWI and (C) DCE imaging, according to the 2015 version of the American College of Radiologists (58)

Score	PZ or TZ
A: T2-weighted imaging	
1	PZ: uniform hyperintens signal intensity (normal); TZ: homogeneous intermediate signal intensity (normal)
2	PZ: linear or wedge-shaped hypointensity or diffuse mild hypointensity, usually indistinct margin; TZ: circumscribed hypointense or heterogeneous encapsulated nodules
3	PZ: heterogeneous signal intensity or non-circumscribed, rounded, moderate hypointensity Includes others that do not qualify as 2, 4 or 5; TZ: heterogeneous signal intensity with obscured margins. Includes others that do not qualify as 2, 4 or 5
4	PZ: circumscribed, homogenous moderate hypointense focus/mass confined to prostate and <1.5 cm in greatest dimension; TZ: lenticular or non-circumscribed, homogeneous moderately hypointense, and <1.5 cm in greatest dimension
5	PZ: same as 4 but ≥1.5 cm in greatest dimension or definite extraprostatic extension/invasive behaviour; TZ: Same as 4 but ≥1.5 cm in greatest dimension or definite extraprostatic extension/invasive behaviour
B: Diffusion-weighted imaging	
1	No abnormality (i.e., normal) on ADC and high b value DWI
2	Indistinct hypointense on ADC
3	Focal mildly/moderately hypointense on ADC and isointense/mildly hyperintense on high b value DWI
4	Focal markedly hypointense on ADC and markedly hyperintense on high b value DWI; <1.5 cm in greatest dimension
5	Same as 4 but ≥1.5 cm in greatest dimension or definite extraprostatic extension (EPE)/invasive behaviour
C: Dynamic contrast enhanced imaging	
–	No early enhancement, or; diffuse enhancement not corresponding to a focal finding on T2 and/or DWI or; focal enhancement corresponding to a lesion demonstrating features of BPH on T2w
+	focal, and; earlier than or contemporaneously with enhancement of adjacent normal prostatic tissues, and; corresponds to suspicious finding on T2w and/or DWI

PIRADS, Prostate Imaging Reporting and Data System; PZ, peripheral zone; TZ, transition zone; ADC, apparent diffusion coefficient; DWI, diffusion weighted imaging.

Table 2 Dominant sequence distribution to PZ and TZ for T2w Imaging and DWI

PZ				TZ				Assessment without adequate DWI (PZ and TZ)				Assessment without adequate DCE (TZ)			
DWI	T2w	DCE	PIRADS	T2w	DWI	DCE	PIRADS	T2w	DWI	DCE	PIRADS	T2w	DWI	DCE	PIRADS
1	Any	Any	1	1	Any	Any	1	1	x	Any	1	1	Any	x	1
2	Any	Any	2	2	Any	Any	2	2	x	Any	2	2	Any	x	2
3	Any	–	3	3	≤4	Any	3	3	x	–	3	3	≤4	x	3
		+	4		5	Any	4		x	+	4		5	x	4
4	Any	Any	4	4	Any	Any	4	4	x	Any	4	4	Any	x	4
5	Any	Any	5	5	Any	Any	5	5	x	Any	5	5	Any	x	5

Any indicates 1-5. PZ, peripheral zone; TZ, transition zone; DWI, diffusion weighted imaging; DCE, dynamic contrast enhanced imaging sequence; PIRADS, Prostate Imaging Reporting and Data System.

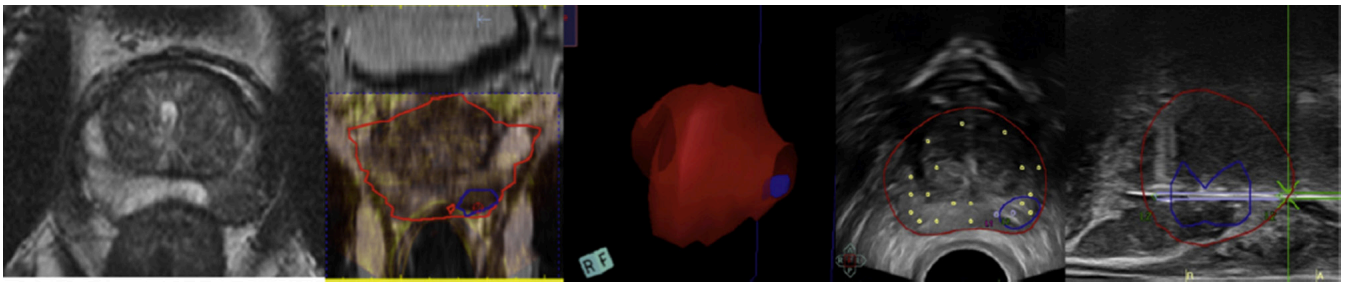

Figure 3 Example of MRI/TRUS-fusion guided biopsy using the MedCom system. MRI-targeted biopsy with ultrasound guidance and software registration. Series showing (from left to right): T2-weighted image showing a low-intensity lesion in the left peripheral zone, delineation of the target volume on the T2-weighted image, a three-dimensional model of prostate volume and target volume, registration of MR volume to ultrasound image, and the biopsy needle within the target volume on the ultrasound image. MRI, magnetic resonance imaging; TRUS, transrectal ultrasound.

to suspicious findings on T2w and/or DWI [*Table 1* (see part C) and *Table 2*] (56).

Technique of MRI targeted biopsy

In general, TB can be performed as direct in-bore MRI-guided biopsy, as VE biopsy or as fusion-biopsy with software-registration. Fusion-guided biopsies consist of co-registrating pre-acquired MRI data with real-time US with the use of software and computing of the probe location and can be performed using elastic fusion systems (e.g., Koelis Urostation, Eigen Artemis) or rigid fusion systems (e.g., Philips Uronav, MedCom BiopSee; *Figure 3*).

Visual estimation

VE allows adaptation of TB in clinical practice without significant upfront cost, but carries a significant learning curve and lacks real-time feedback regarding accuracy (3,19,74). MRI and TRUS images are superimposed by a cognitive overlay of TRUS and MR images during biopsy, using a printed document or by displaying MR images on the screen of a workstation located in the TRUS room, adjacent to the TRUS platform (19). The physician aims the target lesion with knowledge of lesion localization on MRI. Several publications analyzed the value of cognitively performed TB. Lawrentschuk *et al.* detected a higher performance of cognitive TB over random cores, in particular in anterior lesions (75). Haffner *et al.* compared, in a retrospective study, results of TB with those of 12 random biopsies in 555 patients. A TB strategy alone would have necessitated only a mean of 3.8 cores per patient and avoided unnecessary biopsies in 38% of patients with a normal MRI, while avoiding the diagnosis of insignificant cancer detected by random biopsies in 13% cases (18). In this study, 13 significant cancers were missed with TB alone and 12 significant cancers were missed with the standard approach (18). In another study, Puech *et al.* found that MRI prior to biopsy improved CDR which raised from 59% by 12-core SB to 65% by cognitive TB. With regard to significant cancer (Cancer core length >3 mm on any core and GS >3+3) CDR was 67% for TB and 52% for conventional biopsies (35). Labanaris *et al.* showed that TB allow an exact match of biopsy and surgical GS in 90% and concluded that MRI should be performed prior to biopsy to solve underestimation of GS by SB (76). Kasivisvanathan *et al.* detected a statistically not significantly lower CDR of TB (57% cancer detecion rate) compared to a strict reference-test of TPMB (62% CDR) (19). Wysock *et al.* published that VE was slightly inferior to MRI/TRUS-fusion biopsy for all PC (CDR 20.3% *vs.* 32.0%, P=0.1374) and for significant PC (CDR 15.1% *vs.* 26.7%) (74). In conclusion, the currently published studies show an improved accuracy and cancer detection compared to conventional TRUS-biopsy.

In-bore MRI-guided biopsy

The in-bore biopsy approach has the advantages of accurate depiction of needle placement, fewer sampled cores, and a low likelihood of missed targets if these are MRI-visible (20). In-bore biopsy is a targeted biopsy directly performed within the MRI tube. It has the disadvantage of increased cost- and time consumption and the inability to routinely sample the remaining gland (20,21). This is in particular important, as MRI misses app. 10% of significant lesions compared to final RP pathology (15,16). Quentin *et al.* demonstrate an excellent significant cancer detection by in-bore TB of 92.2% (21). In the series of Hoeks *et al.*

265 patients with suspicious lesions on mpMRI with prior negative TRUS-biopsies underwent transrectal in-bore TB, resulting in a CDR of 41% with 87% of these detected cancers found to be clinically significant (20). Multiple studies have corroborated these results, demonstrating that in-bore MRI-guided biopsy is a feasible diagnostic technique in patients with prior negative biopsy, offering a median detection rate of 42%, significantly higher than reported detection rates for repeat SB (22). Pokorny *et al.* demonstrated that an MRI-guided biopsy pathway reduced the diagnosis of low-risk PC by 89.4% and increased the detection of intermediate-risk/high-risk PC by 17.7% (36). However, compared to RP specimen, 14.7% of patients were undergraded by the mpMRI and MRI-guided biopsy approach (36).

MRI/TRUS-fusion-guided biopsy

MR-fusion-guided TB are more often histologically informative and, thus, may overcome the limitations of cognitive TB through reproducible methods for identification of MRI lesions on ultrasound (3,74). Several commercial platforms have become available varying in the method of co-registration and utilizing different hardware platforms for aligning the biopsy with the co-registered image (3,77). MRI/TRUS-fusion-guided biopsy potentially has greater reproducibility due to less operator dependence and by providing real time feedback of actual biopsied locations, compared to VE (3). Disadvantages include higher costs for the software/device, dependence on the software for accuracy, and associated learning curve and operator training (3). Recent publications focused on the detection of PC and of significant disease compared to conventional SB or TPMB as reference-test (4,12,15,26,36,37,78,79). Using the Uronav system and conventional 12-core TRUS-biopsy as reference-test, Siddiqui *et al.* recently demonstrated in a cohort of >1,000 patients that TB diagnosed 30% more high-risk cancers versus standard biopsy (P<0.001) and 17% fewer low-risk cancers (P=0.002) using primary Gleason pattern four as significance level (26). Salami *et al.* and Rastinehad *et al.* used GS ≥3+4 as significant cancer and published that 14.3% to 20.9% of significant PC were detected by TB alone and missed by standard TRUS approach (37,78). Moreover, upgrading from insignificant to significant PC by MRI/TRUS-fusion guided biopsy occurred in 23.5% (37). On the other hand, 4/105 significant PC were missed by MRI/TRUS-fusion guided biopsy (37). Kuru *et al.* and Radtke *et al.* from our group analyzed the detection accuracy of TB compared to a transperineal saturation biopsy as reference-test (12,79). TB detected significantly more PC than SB on per-core analysis (30% *vs.* 8.2%) (79). Analyzing the detection rates of TB versus transperineal SB, TB alone did not lead to a significantly lower detection of significant PC, defined as GS ≥3+4 (P=0.711) (12). At the same time, TB alone avoided overdiagnosis of 43.8% of low-grade tumors (12). Only applying TB in man with suspicious MRI (PIRADS score ≥2) may reduce both, cost and overdetection of low-risk PC, but would have underdiagnosed 11 patients with GS ≥3+4 PC (14.6%) (12). Using RP as reference test, Baco *et al.* demonstrated that 98% of index tumors, defined as the highest GS or biggest volume in case of multifocality with equal GS, were diagnosed by MRI and that the correct location was diagnosed in 98% by MRI/TRUS-fusion guided TB, using the Koelis Urostation (*Figure 4*) (15). However, in the larger prostatetcomy cohort of the Siddiqui publication, the negative predictive value (NPV) of TB to exclude significant disease was only 70%.

Comparative studies of different targeted biopsy approaches

Only a few studies have compared the CDR between different targeting techniques and the results are controversial (5,35,74). In a study comparing VE with two MRI/TRUS-fusion devices, Delongchamps *et al.* reported that cognitive fusion-biopsy was not significantly better than SB, while both software co-registration devices tested (Esaote/MyLabTMTwice and Koelis/Urostation) significantly increased CDR compared to SB using conditional logistic regression analysis in a cohort of 391 patients (5). Wysock *et al.* compared MRI/TRUS-fusion-guided biopsies using the Eigen/Artemis system versus VE targeting in a prospective study including 125 men with suspicious lesions (74). They found that MRI/TRUS-fusion-guided biopsies had a slightly improved CDR compared to VE for aIl cancers (32% *vs.* 26.7%, P=0.1374) and for GS ≥3+4 (20.3% *vs.* 15.1%, P=0.0523). Puech *et al.* observed no difference in the CDR of PC for rigid software co-registration using MedCom Navigator compared to cognitive fusion TB (53% *vs.* 47%) (35). Additionally, no differences were detected for cancer positivity in the subgroups of posterior (46 of 79, 58%), anterior (33 of 79, 42%), or smallest (25 of 79, 32%) MR imaging targets (35).

Targeted versus systematic SB

Several publications investigated the detection accuracy

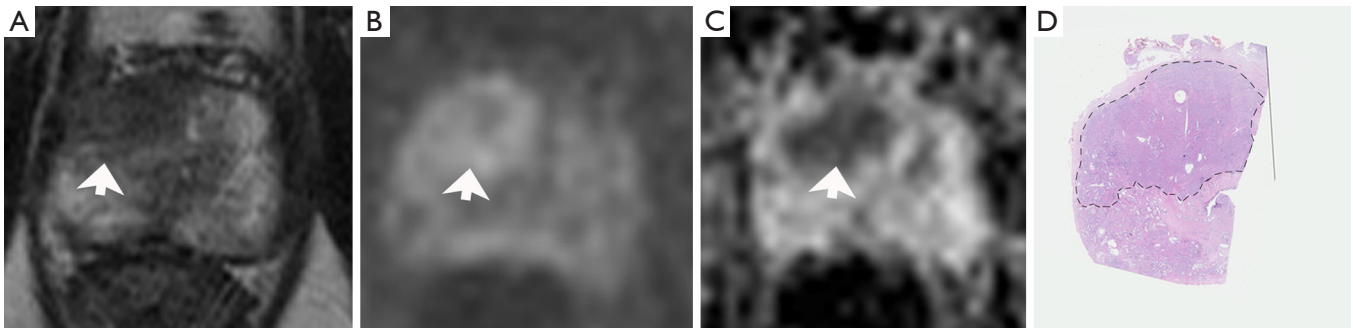

Figure 4 Accuracy of MRI and MRI-targeted biopsy compared to RP specimen. Results of prebiopsy MRI (T2w and DWI is presented) of a 68-year-old male with PSA level 8.1 ng/mL. One negative transrectal prostate biopsy was performed two years before. MRI detected a hypointense area in the right TZon T2w imaging (A, arrow), affecting the AFMS and the anterior horn of the right peripheral zone. Signal intensity was increased on Diffusion-weighted imaging on b value 1,000 sec/mm^2 (B, arrow) with a low signal intensity on ADC map (C, arrow). On biopsy specimen, a GS 4+3 PC occurred in three targeted cores. The patient underwent RP. RP specimen detected a GS 4+3 pT2c PC in the TZ, affecting the AFMS and anterior horn of peripheral zone with negative surgical margins (D, black line). GS, gleason score; DWI, diffusion-weighted imaging; MRI, magnetic resonance imaging; ADC, apparent diffusion coefficient.

of TB and SB alone or in combination (12,26,37,78). As described above, Siddiqui *et al.* from the National Institutes of Health (NIH) analyzed the value of TB *vs.* 12-core TRUS-biopsy in a cohort of 1003 men (26). Additional standard biopsy diagnosed 22% more PC , but 83% of these cases were low-risk PC, while only 5% were high-risk PC (26). The number needed to biopsy with SB in addition to TB to detect one high-risk PC was 200 men (26). Rastinehad *et al.* detected an upgrading from insignificant to significant PC by MRI/TRUS-fusion guided biopsy versus SB in 23.5% (37). On the other hand, only 3.8% of significant PC (defined as GS ≥3+4) were missed by MRI/TRUS-fusion guided biopsy (37). Le *et al.* reported that 17% were diagnosed with GS ≥3+4 PC by 12-core random biopsy alone, whereas 36% of GS ≥3+4 PC were exclusively detected by TB (24).

When MRI/TRUS-fusion guided biopsies are compared to transperineal saturation biopsies, exclusive detection by fusion-guided biopsy occurred in 20.9% of GS ≥3+4 PC and on the other hand in 12.8% by SB alone (12). Valerio *et al.* published in a systematic review of 14 publications, that MRI/TRUS-fusion biopsies detected a median of 9.1% additional clinically significant cancers (range, 5-16.2%) that were missed by standard biopsy alone (53). In contrast, standard biopsies detected a median of 2.1% (range, 0-12.4%) additional clinically significant cancers that were missed by MRI/TRUS-fusion biopsies (53). If the standard biopsy is only a TRUS-biopsy approach, the range of significant PC diagnosted exclusively by standard biopsy stooad at 0-7% (53). In conclusion, Le *et al.* and Radtke *et al.* postulated that the combination of TB and SB represents the reference-standard for cancer detection (12,24). As long as TB miss 3.8-17% of significant PC (according to different definitions of significance), SB should not generally be omitted. Men with suspicion of PC should be counseled and then they may choose if they prefer reduction of overdiagnosis (TB alone) or maximum safety (combination of TB and SB) (12).

Correlation of MRI with surgical pathology

The utility of mpMRI to accurately detect PC and index lesions within the prostate is supported by several studies (15,80-82). An example from our group is given in *Figure 4*. The correlation between histologic lesions and MRI findings is difficult to determine, especially due to the variations between MR sections and prostatectomy slices, and the shrinkage during histopathologic processing of the specimens (80). Correction for this variability has been attempted by using a shrinkage factor, as well as different methods of co-registration between histology and imaging (82-85). However, the tissue shrinkage factor varies among different studies between 1.14 and 1.50 (83). Rosenkrantz *et al.* published one of the first series comparing whole mount sections to mpMRI in 51 patients. They detected a sensitivity and a PPV for an exact match between suspicious lesion on MRI and whole-mount section (belonging to the same region in a 18-sector scheme) in 60.2% and 65.3% of

patients, respectively (81). Regarding approximate matches (discrepancy of up to one region) sensitivity was 75.9% and PPV was 82.6% (81). Turkbey *et al.* published a sensitivity of 80% for the detection of significant PC using T2w Imaging and a sensitivity of 94% for significant lesions in the PZ (82,86). Rud *et al.* used a biparametric MRI (T2w and DWI) to detect the index lesion on consecutive RP, defined as the tumor with EPE, or highest GS, or the largest tumor volume (TV), in that order of priority, in 199 patients (80). In their study, 92% of index lesions and 70% of all lesions were correctly identified by MRI (80). In lesions with TV above 0.5 mL, 86% of cancers were correctly assessed (80). Only 8% of index lesions and 14% of lesions >0.5 mL were missed by MRI (80). In the PIRADS era, Baco *et al.* analyzed the accuracy of mpMRI and MRI/TRUS-fusion guided biopsy in 135 consecutive patients (15). The location of the index lesion was correctly defined in 95% of patients (15). In the remaining 5%, the index tumor was invisible on MRI, but each had a small TV ≤0.4 mL (15). For the MRI-visible index lesions, targeted biopsy-proven PC showed 100% correspondence with the location of the index lesion in RP specimens (15,56,87). The combination of SB and TB detected the index tumor location correctly in 132/135 (98%) of patients (15). Interestingly, both studies demonstrate that the TV of the index lesion was underestimated by MRI (average underestimation 5.9% in Baco *et al.* without utility of a shrinkage factor and 30% in Rud *et al.* with a shrinkage factor of 15%) (15,80). Delongchamps *et al.* analyzed a cohort of 125 consecutive patients, who underwent mpMRI and both, TB and SB and consecutively RP for localized PC (16). MpMRI missed 10% of significant tumor foci on a per-lesion basis but none of the significant PC on a per-patient basis (16). MRI/TRUS-fusion guided TB missed 6% of their targets, resulting in an underdetection of 4% of significant PC (16). Their results suggest that TB alone performed in patients with a suspicious mpMRI would not leave patients undiagnosed with aggressive tumors (16). However, SB in patients with normal mpMRI but increased PSA should not be omitted (16).

MRI in patients with low-risk cancer—utility among men undergoing AS

Accurate risk stratification of patients undergoing AS versus active treatment is crucial for a sound AS program with high patient safety and to reduce potential morbidities associated with radical treatment (88). The most criticized part of AS is its dependence on the initial biopsy quality, since a high number of PC are upgraded in GS after RP (39,89). This cumulates in rather low treatment-free survival rates, although a recently published large cohort study, including 819 patients harboring low-risk PC, has demonstrated excellent results in 10-year (98.1%) and 15-year (94.3%) PC-specific survival.

Accurate and safe stratification means to correctly rule in low-risk disease on the one hand, and to rule out significant PC on the other hand. With regards to AS candidacy, Vargas *et al.* demonstrated that mpMRI can predict upstaging in re-biopsies of AS patients in up to 98% (90,91). Similarly, the utility of MRI/transrectal ultrasound (TRUS)-fusion biopsies in AS cohorts has been demonstrated with encouraging results. Hu *et al.* have shown an upgrading in GS, core involvement and TV of 36% compared to 12-core-TRUS-biopsy (92). Best detection accuracy was demonstrated for the combination of TB and SB, as TB alone led to underdetection of 10% of significant PC (92).

A recently published systematic review focused on mpMRI in AS (93). Schoots *et al.* found an overall reclassification rate of 33% according to PRIAS criteria when TB are used after initial SB (93). In AS follow-up, mpMRI using PIRADS scoring has the potential to rule out significant PC. Mullins *et al.*, Vargas *et al.* and Da Rosa *et al.* showed a NPV of above 90% for a pristine MRI to rule out significant PC (90,94,95).

Thus, Schoots *et al.* conclude that MRI can detect clinically significant disease in one third to half of men at the start of surveillance and in the follow-up course (93). However, at the moment no robust data are available to support the use of MRI in place of repeat biopsy to detect progression over time (93).

The role of MRI in risk stratification and prediction of ECE and RP outcome

MpMRI has demonstrated excellent accuracy in index lesion detection, compared to RP specimens described by recent publications. However, risk group stratification for localized PC, as defined by NCCN criteria incorporates serum PSA-level, the GS of biopsy specimen and the clinical T-stage based on digital rectal examination (DRE) and lacks formal mpMRI incorporation (96).

In the 2012 ESUR guidelines a scoring system for extracapsular disease was published, including criteria regarding ECE, seminal vesicle infiltration (SV), adjacent and infiltration of distal sphincter and bladder neck (*Table 3*, *Figure 5*) (9).

Somford *et al.* validated the ESUR scoring system in a

Table 3 ESUR scoring of extraprostatic disease, according to ESUR prostate MR guidelines (9)

Criteria	Findings	Score
Extra-capsular extension	Abutment	1
	Irregularity	3
	Neurovascular bundle thickening	4
	Bulge, loss of capsule	4
	Measurable extra-capsular disease	5
Seminal vesicles	Expansion	1
	Low T2 signal	2
	Filling in of angle	3
	Enhancement and impeded diffusion	4
Distal sphincter	Adjacent tumour	3
	Effacement of low signal sphincter muscle	3
	Abnormal enhancement extending into sphincter	4
Bladder neck	Adjacent tumour	2
	Loss of low T2 signal in bladder muscle	3
	Abnormal enhancement extending into bladder neck	4

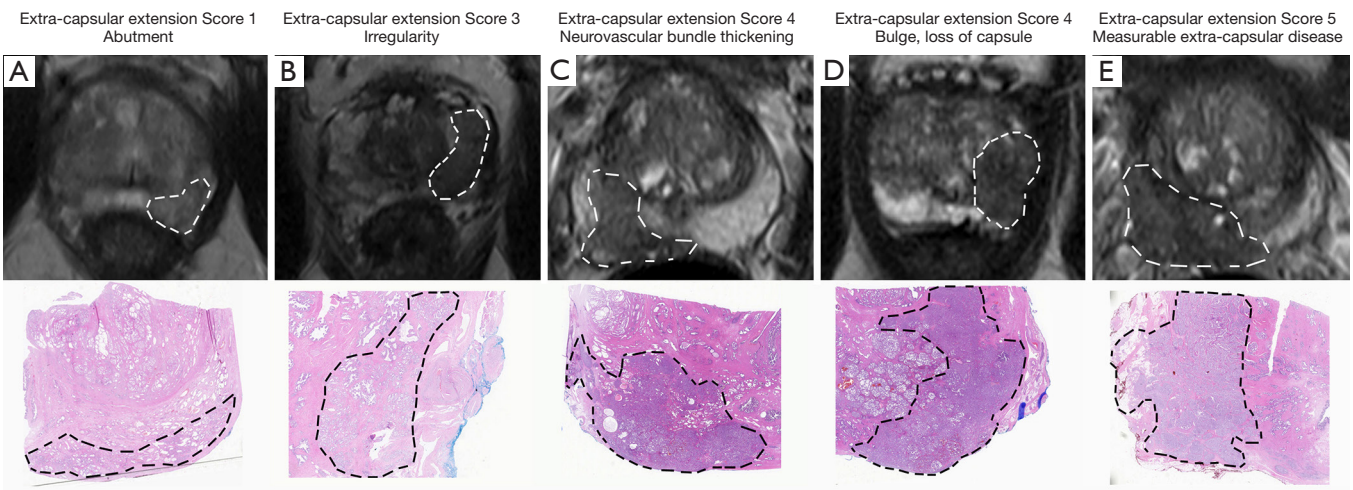

Figure 5 Figures are demonstrating the ESUR ECE-score on mpMRI (T2w Imaging) and histopathologic correlations for every level (9): (A) ESUR extra-capsular extension Score 1—Abutment; (B) ESUR extra-capsular extension Score 3—Irregularity; (C) ESUR extra-capsular extension Score 4—Neurovascular bundle thickening; (D) ESUR extra-capsular extension Score 4—Bulge, loss of capsule; (E) ESUR extra-capsular extension Score 5—Measureable extra-capsular disease. ESUR, the European Society of Urogenital Radiology; ECE, extracapsular extension.

cohort of 183 patients and found a NPV of 87.7% for ECE in patients with low-risk PC and a PPV for ECE in high-risk patients of 88.8% (28). This was slightly higher than an already excellent PPV in the studies of Cornud et al and Rud *et al.* (97,98). Marcus *et al.* investigated the impact of preoperative MRI on NCCN risk group classification in a cohort of 71 patients and found that 16.9% of patients were upstaged by MRI, mostly (83.3% of these subgroups) from intermediate- to high-risk (29). Additionally, the treatment regime was changed in 8.5% due to presurgical MRI (29). McClure *et al.* focused on differences between the initial surgical plan, according to D'Amico risk stratification, and the performed RP with knowledge of the presurgical MRI (99). They found a change in the initial surgical plan in 27% of patients, analyzing a cohort of 104 consecutive men (99). In their study, the surgical plan was changed to a nerve-sparing

technique in 61% and to a non-nerve-sparing in 39% (99). Wang *et al.* and Sala *et al.* from Memorial-Sloan-Kettering Cancer Center developed a score for ECE and seminal vesicle invasion that is analogous to the PIRADS score published by the ESUR (100,101). They found an AUC of 0.76 for MRI to predict seminal vesicle invasion. When the MRI score was compared to a Kattan nomogram, the combination of both significantly increased the AUC (AUC 0.86 versus AUC 0.80 for Kattan nomogram, P<0.05) (100). Sala *et al.* reported an AUC of 0.87 for prediction of ECE in a cohort of 45 patients how underwent salvage RP (101).

In contrast to clinical parameters like NCCN criteria, prostate MRI offers localized staging and allows the surgeon to sculpt the extent of PC and possible ECE (102). Another decision-making tool is maximum capsule contact length on MRI. Baco *et al.* analyzed the predictive value of MRI-determined tumor contact length to the capsule and found a correlation between ECE and tumor contact length of r=0.839 (P<0.001) using Spearman's regression (103). Based on ROC curve analysis, the best threshold of MRI determined tumor contact length was 20 mm (103).

In conclusion, MR imaging can potentially improve the accuracy of the surgeon's decision to resect or preserve the neurovascular bundle in patients undergoing RP (102).

Conclusions

MpMRI represents a potential tool to overcome limitations of conventional TRUS-biopsy. The established PIRADS scores make mpMRI generalizable and reproducible. Compared to the gold-standard of RP, MRI detects app. 90% of significant index lesions correctly, but TV is currently underestimated. Several techniques of TB are available and the optimal method has not yet been established. The encouraging results of in-bore TB and MRI/TRUS-fusion guided biopsies may outperform VE. TB detect significantly more significant PC compared to SB and are non-inferior compared to TPMB as reference test. However, as long as TB miss around 5-15% of significant PC (according to different definitions of significance), SB should not be omitted, especially in patients without previous biopsy. Among patients under AS, mpMRI helps to confirm AS eligibility, by correct prediction of upstaging in re-biopsies of AS patients and by accurately ruling-out significant PC. The future role of mpMRI in the presurgical setting of RP is emerging, as mpMRI can help to change the initial surgical plan, according to clinical decision making, in up to 30% of cases. Before wide incorporation of mpMRI, further comparative studies, including randomized multicenter studies, and evaluation of cost-effectiveness are necessary, but potential cost-saving approaches like biparametric MRI are in the starting gates. Additionally the role of molecular imaging, e.g., PSMA-PET-CT/MRI, might provide ancillary information on tumor characterization and PC aggressiveness, and its role will be depicted in further publications (104,105).

Acknowledgements

M Hohenfellner and BA Hadaschik receive funding from the German Cancer Aid. BA Hadaschik is grateful for funding from the German Research Foundation and the European Foundation of Urology.

Footnote

Conflicts of Interest: The authors have no conflicts of interest to declare.

References

1. Jemal A, Bray F, Center MM, et al. Global cancer statistics. CA Cancer J Clin 2011;61:69-90.
2. Heidenreich A, Bastian PJ, Bellmunt J, et al. EAU guidelines on prostate cancer. part 1: screening, diagnosis, and local treatment with curative intent-update 2013. Eur Urol 2014;65:124-37.
3. Bjurlin MA, Meng X, Le Nobin J, et al. Optimization of prostate biopsy: the role of magnetic resonance imaging targeted biopsy in detection, localization and risk assessment. J Urol 2014;192:648-58.
4. Siddiqui MM, Rais-Bahrami S, Truong H, et al. Magnetic resonance imaging/ultrasound-fusion biopsy significantly upgrades prostate cancer versus systematic 12-core transrectal ultrasound biopsy. Eur Urol 2013;64:713-9.
5. Delongchamps NB, Peyromaure M, Schull A, et al. Prebiopsy magnetic resonance imaging and prostate cancer detection: comparison of random and targeted biopsies. J Urol 2013;189:493-9.
6. Hamoen EH, de Rooij M, Witjes JA, et al. Use of the Prostate Imaging Reporting and Data System (PI-RADS) for Prostate Cancer Detection with Multiparametric Magnetic Resonance Imaging: A Diagnostic Meta-analysis. Eur Urol 2015;67:1112-21.
7. Delongchamps NB, Rouanne M, Flam T, et al. Multiparametric magnetic resonance imaging for the detection and localization of prostate cancer: combination

of T2-weighted, dynamic contrast-enhanced and diffusion-weighted imaging. BJU Int 2011;107:1411-8.
8. Dickinson L, Ahmed HU, Allen C, et al. Scoring systems used for the interpretation and reporting of multiparametric MRI for prostate cancer detection, localization, and characterization: could standardization lead to improved utilization of imaging within the diagnostic pathway? J Magn Reson Imaging 2013;37:48-58.
9. Barentsz JO, Richenberg J, Clements R, et al. ESUR prostate MR guidelines 2012. Eur Radiol 2012;22:746-57.
10. Portalez D, Mozer P, Cornud F, et al. Validation of the European Society of Urogenital Radiology scoring system for prostate cancer diagnosis on multiparametric magnetic resonance imaging in a cohort of repeat biopsy patients. Eur Urol 2012;62:986-96.
11. Kuru TH, Roethke MC, Rieker P, et al. Histology core-specific evaluation of the European Society of Urogenital Radiology (ESUR) standardised scoring system of multiparametric magnetic resonance imaging (mpMRI) of the prostate. BJU Int 2013;112:1080-7.
12. Radtke JP, Kuru TH, Boxler S, et al. Comparative analysis of transperineal template saturation prostate biopsy versus magnetic resonance imaging targeted biopsy with magnetic resonance imaging-ultrasound fusion guidance. J Urol 2015;193:87-94.
13. Thompson JE, Moses D, Shnier R, et al. Multiparametric magnetic resonance imaging guided diagnostic biopsy detects significant prostate cancer and could reduce unnecessary biopsies and over detection: a prospective study. J Urol 2014;192:67-74.
14. Isebaert S, Van den Bergh L, Haustermans K, et al. Multiparametric MRI for prostate cancer localization in correlation to whole-mount histopathology. J Magn Reson Imaging 2013;37:1392-401.
15. Baco E, Ukimura O, Rud E, et al. Magnetic resonance imaging-transectal ultrasound image-fusion biopsies accurately characterize the index tumor: correlation with step-sectioned radical prostatectomy specimens in 135 patients. Eur Urol 2015;67:787-94.
16. Delongchamps NB, Lefèvre A, Bouazza N, et al. Detection of Significant Prostate Cancer with Magnetic Resonance Targeted Biopsies-Should Transrectal Ultrasound-Magnetic Resonance Imaging Fusion Guided Biopsies Alone be a Standard of Care? J Urol 2015;193:1198-204.
17. Le JD, Tan N, Shkolyar E, et al. Multifocality and prostate cancer detection by multiparametric magnetic resonance imaging: correlation with whole-mount histopathology. Eur Urol 2015;67:569-76.
18. Haffner J, Lemaitre L, Puech P, et al. Role of magnetic resonance imaging before initial biopsy: comparison of magnetic resonance imaging-targeted and systematic biopsy for significant prostate cancer detection. BJU Int 2011;108:E171-8.
19. Kasivisvanathan V, Dufour R, Moore CM, et al. Transperineal magnetic resonance image targeted prostate biopsy versus transperineal template prostate biopsy in the detection of clinically significant prostate cancer. J Urol 2013;189:860-6.
20. Hoeks CM, Schouten MG, Bomers JG, et al. Three-Tesla magnetic resonance-guided prostate biopsy in men with increased prostate-specific antigen and repeated, negative, random, systematic, transrectal ultrasound biopsies: detection of clinically significant prostate cancers. Eur Urol 2012;62:902-9.
21. Quentin M, Blondin D, Arsov C, et al. Prospective evaluation of magnetic resonance imaging guided in-bore prostate biopsy versus systematic transrectal ultrasound guided prostate biopsy in biopsy naïve men with elevated prostate specific antigen. J Urol 2014;192:1374-9.
22. Overduin CG, Fütterer JJ, Barentsz JO. MRI-guided biopsy for prostate cancer detection: a systematic review of current clinical results. Curr Urol Rep 2013;14:209-13.
23. Bains LJ, Studer UE, Froehlich JM, et al. Diffusion-weighted magnetic resonance imaging detects significant prostate cancer with high probability. J Urol 2014;192:737-42.
24. Le JD, Stephenson S, Brugger M, et al. Magnetic resonance imaging-ultrasound fusion biopsy for prediction of final prostate pathology. J Urol 2014;192:1367-73.
25. Ukimura O, Coleman JA, de la Taille A, et al. Contemporary role of systematic prostate biopsies: indications, techniques, and implications for patient care. Eur Urol 2013;63:214-30.
26. Siddiqui MM, Rais-Bahrami S, Turkbey B, et al. Comparison of MR/ultrasound fusion-guided biopsy with ultrasound-guided biopsy for the diagnosis of prostate cancer. JAMA 2015;313:390-7.
27. Moore CM, Kasivisvanathan V, Eggener S, et al. Standards of reporting for MRI-targeted biopsy studies (START) of the prostate: recommendations from an International Working Group. Eur Urol 2013;64:544-52.
28. Somford DM, Hamoen EH, Fütterer JJ, et al. The predictive value of endorectal 3 Tesla multiparametric magnetic resonance imaging for extraprostatic extension in patients with low, intermediate and high risk prostate cancer. J Urol 2013;190:1728-34.
29. Marcus DM, Rossi PJ, Nour SG, et al. The impact of multiparametric pelvic magnetic resonance imaging on risk stratification in patients with localized prostate cancer.

Urology 2014;84:132-7.
30. Serefoglu EC, Altinova S, Ugras NS, et al. How reliable is 12-core prostate biopsy procedure in the detection of prostate cancer? Can Urol Assoc J 2012:1-6.
31. Mygatt J, Sesterhenn I, Rosner I, et al. Anterior tumors of the prostate: clinicopathological features and outcomes. Prostate Cancer Prostatic Dis 2014;17:75-80.
32. Nevoux P, Ouzzane A, Ahmed HU, et al. Quantitative tissue analyses of prostate cancer foci in an unselected cystoprostatectomy series. BJU Int 2012;110:517-23.
33. Epstein JI, Walsh PC, Carmichael M, et al. Pathologic and clinical findings to predict tumor extent of nonpalpable (stage T1c) prostate cancer. JAMA 1994;271:368-74.
34. Wolters T, Montironi R, Mazzucchelli R, et al. Comparison of incidentally detected prostate cancer with screen-detected prostate cancer treated by prostatectomy. Prostate 2012;72:108-15.
35. Puech P, Rouvière O, Renard-Penna R, et al. Prostate cancer diagnosis: multiparametric MR-targeted biopsy with cognitive and transrectal US-MR fusion guidance versus systematic biopsy--prospective multicenter study. Radiology 2013;268:461-9.
36. Pokorny MR, de Rooij M, Duncan E, et al. Prospective study of diagnostic accuracy comparing prostate cancer detection by transrectal ultrasound-guided biopsy versus magnetic resonance (MR) imaging with subsequent MR-guided biopsy in men without previous prostate biopsies. Eur Urol 2014;66:22-9.
37. Rastinehad AR, Turkbey B, Salami SS, et al. Improving detection of clinically significant prostate cancer: magnetic resonance imaging/transrectal ultrasound fusion guided prostate biopsy. J Urol 2014;191:1749-54.
38. Dinh KT, Mahal BA, Ziehr DR, et al. Incidence and Predictors of Upgrading and Up Staging Among 10,000 Contemporary Patients with Low Risk Prostate Cancer. J Urol 2015. [Epub ahead of print].
39. Shaw GL, Thomas BC, Dawson SN, et al. Identification of pathologically insignificant prostate cancer is not accurate in unscreened men. Br J Cancer 2014;110:2405-11.
40. Zlotta AR, Egawa S, Pushkar D, et al. Prevalence of prostate cancer on autopsy: cross-sectional study on unscreened Caucasian and Asian men. J Natl Cancer Inst 2013;105:1050-8.
41. Cooperberg MR, Broering JM, Kantoff PW, et al. Contemporary trends in low risk prostate cancer: risk assessment and treatment. J Urol 2007;178:S14-9.
42. Schröder FH. Landmarks in prostate cancer screening. BJU Int 2012;110 Suppl 1:3-7.
43. Loeb S, Carter HB, Berndt SI, et al. Complications after prostate biopsy: data from SEER-Medicare. J Urol 2011;186:1830-4.
44. Lundström KJ, Drevin L, Carlsson S, et al. Nationwide population based study of infections after transrectal ultrasound guided prostate biopsy. J Urol 2014;192:1116-22.
45. Loeb S, Vellekoop A, Ahmed HU, et al. Systematic review of complications of prostate biopsy. Eur Urol 2013;64:876-92.
46. Feliciano J, Teper E, Ferrandino M, et al. The incidence of fluoroquinolone resistant infections after prostate biopsy--are fluoroquinolones still effective prophylaxis? J Urol 2008;179:952-5; discussion 955.
47. Cohen JE, Landis P, Trock BJ, et al. Fluoroquinolone resistance in the rectal carriage of men in an active surveillance cohort: longitudinal analysis. J Urol 2015;193:552-6.
48. Crawford ED, Rove KO, Barqawi AB, et al. Clinical-pathologic correlation between transperineal mapping biopsies of the prostate and three-dimensional reconstruction of prostatectomy specimens. Prostate 2013;73:778-87.
49. Ploussard G, Nicolaiew N, Marchand C, et al. Prospective evaluation of an extended 21-core biopsy scheme as initial prostate cancer diagnostic strategy. Eur Urol 2014;65:154-61.
50. Onik G, Miessau M, Bostwick DG. Three-dimensional prostate mapping biopsy has a potentially significant impact on prostate cancer management. J Clin Oncol 2009;27:4321-6.
51. Ahmed HU, Hu Y, Carter T, et al. Characterizing clinically significant prostate cancer using template prostate mapping biopsy. J Urol 2011;186:458-64.
52. Lecornet E, Ahmed HU, Hu Y, et al. The accuracy of different biopsy strategies for the detection of clinically important prostate cancer: a computer simulation. J Urol 2012;188:974-80.
53. Valerio M, Donaldson I, Emberton M, et al. Detection of Clinically Significant Prostate Cancer Using Magnetic Resonance Imaging-Ultrasound Fusion Targeted Biopsy: A Systematic Review. Eur Urol 2015;68:8-19.
54. Hricak H, Williams RD, Spring DB, et al. Anatomy and pathology of the male pelvis by magnetic resonance imaging. AJR Am J Roentgenol 1983;141:1101-10.
55. Raskolnikov D, George AK, Rais-Bahrami S, et al. Multiparametric magnetic resonance imaging and image-guided biopsy to detect seminal vesicle invasion by prostate cancer. J Endourol 2014;28:1283-9.
56. American College of Radiology. MR Prostate Imaging Reporting and Data System version 2.0. Accessed June 2015. Available online: http://www.acr.org/Quality-Safety/

Resources/PIRADS/
57. McNeal JE. The zonal anatomy of the prostate. Prostate 1981;2:35-49.
58. Bouyé S, Potiron E, Puech P, et al. Transition zone and anterior stromal prostate cancers: zone of origin and intraprostatic patterns of spread at histopathology. Prostate 2009;69:105-13.
59. Hricak H, Dooms GC, McNeal JE, et al. MR imaging of the prostate gland: normal anatomy. AJR Am J Roentgenol 1987;148:51-8.
60. Wang L, Mazaheri Y, Zhang J, et al. Assessment of biologic aggressiveness of prostate cancer: correlation of MR signal intensity with Gleason grade after radical prostatectomy. Radiology 2008;246:168-76.
61. Chesnais AL, Niaf E, Bratan F, et al. Differentiation of transitional zone prostate cancer from benign hyperplasia nodules: evaluation of discriminant criteria at multiparametric MRI. Clin Radiol 2013;68:e323-30.
62. Hoeks CM, Hambrock T, Yakar D, et al. Transition zone prostate cancer: detection and localization with 3-T multiparametric MR imaging. Radiology 2013;266:207-17.
63. Akin O, Sala E, Moskowitz CS, et al. Transition zone prostate cancers: features, detection, localization, and staging at endorectal MR imaging. Radiology 2006;239:784-92.
64. Katahira K, Takahara T, Kwee TC, et al. Ultra-high-b value diffusion-weighted MR imaging for the detection of prostate cancer: evaluation in 201 cases with histopathological correlation. Eur Radiol 2011;21:188-96.
65. Mazaheri Y, Vargas HA, Akin O, et al. Reducing the influence of b value selection on diffusion-weighted imaging of the prostate: evaluation of a revised monoexponential model within a clinical setting. J Magn Reson Imaging 2012;35:660-8.
66. Rosenkrantz AB, Triolo MJ, Melamed J, et al. Whole-lesion apparent diffusion coefficient metrics as a marker of percentage Gleason 4 component within Gleason 7 prostate cancer at radical prostatectomy. J Magn Reson Imaging 2015;41:708-14.
67. Turkbey B, Shah VP, Pang Y, et al. Is apparent diffusion coefficient associated with clinical risk scores for prostate cancers that are visible on 3-T MR images? Radiology 2011;258:488-95.
68. Collins DJ, Padhani AR. Dynamic magnetic resonance imaging of tumor perfusion. Approaches and biomedical challenges. IEEE Eng Med Biol Mag 2004;23:65-83.
69. Hara N, Okuizumi M, Koike H, et al. Dynamic contrast-enhanced magnetic resonance imaging (DCE-MRI) is a useful modality for the precise detection and staging of early prostate cancer. Prostate 2005;62:140-7.
70. Yoshizako T, Wada A, Hayashi T, et al. Usefulness of diffusion-weighted imaging and dynamic contrast-enhanced magnetic resonance imaging in the diagnosis of prostate transition-zone cancer. Acta Radiol 2008;49:1207-13.
71. Rosenkrantz AB, Kim S, Campbell N, et al. Transition zone prostate cancer: revisiting the role of multiparametric MRI at 3 T. AJR Am J Roentgenol 2015;204:W266-72.
72. Schimmöller L, Quentin M, Arsov C, et al. MR-sequences for prostate cancer diagnostics: validation based on the PI-RADS scoring system and targeted MR-guided in-bore biopsy. Eur Radiol 2014;24:2582-9.
73. Rais-Bahrami S, Siddiqui MM, Vourganti S, et al. Diagnostic value of biparametric magnetic resonance imaging (MRI) as an adjunct to prostate-specific antigen (PSA)-based detection of prostate cancer in men without prior biopsies. BJU Int 2015;115:381-8.
74. Wysock JS, Rosenkrantz AB, Huang WC, et al. A prospective, blinded comparison of magnetic resonance (MR) imaging-ultrasound fusion and visual estimation in the performance of MR-targeted prostate biopsy: the PROFUS trial. Eur Urol 2014;66:343-51.
75. Lawrentschuk N, Haider MA, Daljeet N, et al. 'Prostatic evasive anterior tumours': the role of magnetic resonance imaging. BJU Int 2010;105:1231-6.
76. Labanaris AP, Zugor V, Smiszek R, et al. Guided e-MRI prostate biopsy can solve the discordance between Gleason score biopsy and radical prostatectomy pathology. Magn Reson Imaging 2010;28:943-6.
77. Cornud F, Brolis L, Delongchamps NB, et al. TRUS-MRI image registration: a paradigm shift in the diagnosis of significant prostate cancer. Abdom Imaging 2013;38:1447-63.
78. Salami SS, Ben-Levi E, Yaskiv O, et al. In patients with a previous negative prostate biopsy and a suspicious lesion on magnetic resonance imaging, is a 12-core biopsy still necessary in addition to a targeted biopsy? BJU Int 2015;115:562-70.
79. Kuru TH, Roethke MC, Seidenader J, et al. Critical evaluation of magnetic resonance imaging targeted, transrectal ultrasound guided transperineal fusion biopsy for detection of prostate cancer. J Urol 2013;190:1380-6.
80. Rud E, Klotz D, Rennesund K, et al. Detection of the index tumour and tumour volume in prostate cancer using T2-weighted and diffusion-weighted magnetic resonance imaging (MRI) alone. BJU Int 2014;114:E32-42.
81. Rosenkrantz AB, Deng FM, Kim S, et al. Prostate cancer: multiparametric MRI for index lesion localization--a multiple-reader study. AJR Am J Roentgenol 2012;199:830-7.
82. Turkbey B, Pinto PA, Mani H, et al. Prostate cancer: value of multiparametric MR imaging at 3 T for detection--

histopathologic correlation. Radiology 2010;255:89-99.
83. Schned AR, Wheeler KJ, Hodorowski CA, et al. Tissue-shrinkage correction factor in the calculation of prostate cancer volume. Am J Surg Pathol 1996;20:1501-6.
84. Orczyk C, Taneja SS, Rusinek H, et al. Assessment of change in prostate volume and shape following surgical resection through co-registration of in-vivo MRI and fresh specimen ex-vivo MRI. Clin Radiol 2014;69:e398-403.
85. Haider MA, van der Kwast TH, Tanguay J, et al. Combined T2-weighted and diffusion-weighted MRI for localization of prostate cancer. AJR Am J Roentgenol 2007;189:323-8.
86. Turkbey B, Mani H, Shah V, et al. Multiparametric 3T prostate magnetic resonance imaging to detect cancer: histopathological correlation using prostatectomy specimens processed in customized magnetic resonance imaging based molds. J Urol 2011;186:1818-24.
87. Dickinson L, Ahmed HU, Allen C, et al. Magnetic resonance imaging for the detection, localisation, and characterisation of prostate cancer: recommendations from a European consensus meeting. Eur Urol 2011;59:477-94.
88. Loeb S, Bjurlin MA, Nicholson J, et al. Overdiagnosis and overtreatment of prostate cancer. Eur Urol 2014;65:1046-55.
89. Epstein JI, Feng Z, Trock BJ, et al. Upgrading and downgrading of prostate cancer from biopsy to radical prostatectomy: incidence and predictive factors using the modified Gleason grading system and factoring in tertiary grades. Eur Urol 2012;61:1019-24.
90. Vargas HA, Akin O, Afaq A, et al. Magnetic resonance imaging for predicting prostate biopsy findings in patients considered for active surveillance of clinically low risk prostate cancer. J Urol 2012;188:1732-8.
91. van den Bergh RC, Roemeling S, Roobol MJ, et al. Outcomes of men with screen-detected prostate cancer eligible for active surveillance who were managed expectantly. Eur Urol 2009;55:1-8.
92. Hu JC, Chang E, Natarajan S, et al. Targeted prostate biopsy in select men for active surveillance: do the Epstein criteria still apply? J Urol 2014;192:385-90.
93. Schoots IG, Petrides N, Giganti F, et al. Magnetic resonance imaging in active surveillance of prostate cancer: a systematic review. Eur Urol 2015;67:627-36.
94. Mullins JK, Bonekamp D, Landis P, et al. Multiparametric magnetic resonance imaging findings in men with low-risk prostate cancer followed using active surveillance. BJU Int 2013;111:1037-45.
95. Da Rosa MR, Milot L, Sugar L, et al. A prospective comparison of MRI-US fused targeted biopsy versus systematic ultrasound-guided biopsy for detecting clinically significant prostate cancer in patients on active surveillance. J Magn Reson Imaging 2015;41:220-5.
96. Cheney VT. Prostate cancer. Lancet 1994;343:976-7.
97. Cornud F, Rouanne M, Beuvon F, et al. Endorectal 3D T2-weighted 1mm-slice thickness MRI for prostate cancer staging at 1.5Tesla: should we reconsider the indirects signs of extracapsular extension according to the D'Amico tumor risk criteria? Eur J Radiol 2012;81:e591-7.
98. Rud E, Klotz D, Rennesund K, et al. Preoperative magnetic resonance imaging for detecting uni- and bilateral extraprostatic disease in patients with prostate cancer. World J Urol 2015;33:1015-21.
99. McClure TD, Margolis DJ, Reiter RE, et al. Use of MR imaging to determine preservation of the neurovascular bundles at robotic-assisted laparoscopic prostatectomy. Radiology 2012;262:874-83.
100. Wang L, Hricak H, Kattan MW, et al. Combined endorectal and phased-array MRI in the prediction of pelvic lymph node metastasis in prostate cancer. AJR Am J Roentgenol 2006;186:743-8.
101. Sala E, Eberhardt SC, Akin O, et al. Endorectal MR imaging before salvage prostatectomy: tumor localization and staging. Radiology 2006;238:176-83.
102. Hricak H, Wang L, Wei DC, et al. The role of preoperative endorectal magnetic resonance imaging in the decision regarding whether to preserve or resect neurovascular bundles during radical retropubic prostatectomy. Cancer 2004;100:2655-63.
103. Baco E, Rud E, Vlatkovic L, et al. Predictive Value of Magnetic Resonance Imaging Determined Tumor Contact Length for Extracapsular Extension of Prostate Cancer. J Urol 2015;193:466-72.
104. Eiber M, Nekolla SG, Maurer T, et al. 68 Ga-PSMA PET/MR with multimodality image analysis for primary prostate cancer. 2014. Available online: http://link.springer.com/article/10.1007%2Fs00261-014-0301-z
105. Roethke MC, Kuru TH, Afshar-Oromieh A, et al. Hybrid positron emission tomography-magnetic resonance imaging with gallium 68 prostate-specific membrane antigen tracer: a next step for imaging of recurrent prostate cancer-preliminary results. Eur Urol 2013;64:862-4.

Cite this article as: Radtke JP, Teber D, Hohenfellner M, Hadaschik BA. The current and future role of magnetic resonance imaging in prostate cancer detection and management. Transl Androl Urol 2015;4(3):326-341. doi: 10.3978/j.issn.2223-4683.2015.06.05

